Journal of Applied Polymer Science

WILEY

Applied Polymer SCIENCE

RESEARCH ARTICLE OPEN ACCESS

Influence of Six Plasticizers on the Morphology, Crystallinity, and Thermal Properties of Poly(Vinylidene Difluoride) Films

Anya Sonnendecker | Matome W. Mametja | Johan Labuschagne (FJWJ)

Department of Chemical Engineering, Faculty of Engineering, Built Environment & IT, University of Pretoria, Pretoria, South Africa

Correspondence: Anya Sonnendecker (abezuidenhoudt89@gmail.com)

Received: 12 November 2024 | **Revised:** 7 April 2025 | **Accepted:** 12 April 2025

Funding: This study was financially supported by funding from the Fluorochemistry Expansion Initiative (FEI) that was managed by the South African Department of Science and Technology (DST) and from the Council for Scientific and Industrial Research (CSIR), South Africa.

Keywords: films | morphology | plasticizer | spectroscopy | thermal properties

ABSTRACT

Poly(vinylidene fluoride) (PVDF) is renowned for its durability but suffers from limited flexibility, restricting its use as a protective topcoat on architectural textiles. This study investigated six ester-based plasticizers at a loading of 50 wt% in a 10 wt% PVDF solution (dissolved in dimethylacetamide at 50°C) to identify an optimal candidate for enhancing flexibility while maintaining suitable morphology. DSC indicated that P3 (dibutyl phthalate) lowered the polymer's melting temperature to 154°C (from 170°C for pure PVDF) and decreased its glass transition temperature (T_g) to −81.5°C. However, SEM revealed significant porosity, undermining its protective function. In contrast, P2 (di(propylene glycol)dibenzoate) resulted in a 10°C reduction in melting temperature and a 19°C reduction in crystallization temperature, yet only increased T_g by 3°C; the film remained more flexible than unmodified PVDF. SEM confirmed minimal voids, indicating good compatibility. Furthermore, DSC data demonstrated P2 raised the degree of crystallinity from 31% in the reference film to 34% while preserving structural integrity. These findings highlight P2 as the most viable plasticizer for producing flexible PVDF topcoats, offering a simpler, cost-effective solution with the potential to extend the lifespan of architectural textiles in under-resourced regions.

1 | Introduction

Poly(vinylidene fluoride) (PVDF) is a semi-crystalline polymer renowned for its exceptional properties and usage in a wide array of industrial applications [1]. However, PVDF's inherent rigidity limits its usage in applications that require flexibility, particularly as a protective topcoat on flexible architectural textiles, a field that has grown significantly over the past decade [2].

Although advancements in polymer chemistry have enabled the synthesis of flexible PVDF copolymers, expanding their applicability to flexible substrates [3–6], they often require sophisticated infrastructure, which may be lacking or too expensive for underdeveloped regions. This limitation underscores the necessity for alternative approaches to enhance the flexibility of PVDF without relying on complex copolymerization processes. The current research forms part of a larger project whose aim is to aid in the construction of affordable housing within underdeveloped regions by making use of architectural textiles. However, non-UV-protected textiles have a very short lifespan; hence the need for the development of a less expensive PVDF-based protective topcoat.

As an alternative to the creation of complex copolymers, the addition of plasticizers could be considered to enhance PVDF's flexibility. Plasticizers typically function by interposing

themselves between the polymer chains, hindering tight chain packing during crystallization and thereby increasing polymer flexibility [7, 8].

Despite the potential of plasticizers to modify PVDF's flexibility, there is a scarcity of research focused on identifying effective plasticizers specifically for the production of uniform, high-quality thin films. Most of the research available focuses on plasticizers, or more aptly named diluents, used in the melt processing of PVDF [9], in the creation of membranes for filtration [10], in the optimization of PVDF's piezoelectric properties [11–13], or their effects on the mechanical properties of hard elastic fibers [11]. Hence, there is a specific need for a plasticizer that would improve the flexibility of high molecular weight PVDF in the production of thin films.

A patent published by [14] provided some guidance on selecting a viable. The patent proposed that PVDF's flexibility could be augmented by adding specific esters as plasticizers. The patent provided a list of viable esters. Nonetheless, the influence of these esters on the morphology and physical properties of high molecular weight PVDF thin films remains unexplored. The six different plasticizers used in the current research were selected from the list of potential esters provided in the patent.

The primary aim of this research was to identify the most suitable plasticizer that not only enhances the flexibility of PVDF-based thin films but also yields a thin film with a surface morphology that would serve as an acceptable protective UV-resistant topcoat for flexible architectural textiles. To achieve this aim, six different plasticized PVDF thin films were produced using the solution casting method. Comprehensive analyses were conducted using Fourier-transform infrared spectroscopy (FTIR) to assess crystalline phases, dynamic mechanical thermal analysis (DMTA), and differential scanning calorimetry (DSC) to evaluate thermal properties, and scanning electron microscopy (SEM) to examine film morphology. The experimental results were systematically assessed to determine the impact of each plasticizer on the structural and physical characteristics of the PVDF thin films, thereby identifying the most effective plasticizers for producing flexible, high-performance PVDF thin films.

This study provides a new perspective into a previously unexplored research space by providing a systematic evaluation of a range of potential plasticizers specifically for high molecular weight PVDF thin film production with possible applications in flexible coating development. It is the first to deliver the impact of several different ester-based plasticizers on both the thermal and morphological performance of PVDF thin films.

2 | Experimental

2.1 | Raw Materials

Solef 6020\1001 powder was procured from A. Schulman (now owned by LyondellBasell) to be used as raw material for this investigation. Solef 6020/1001 possesses a melt flow index of 2 g/10 min (measured at 230°C under a 21.6 kg load). DMAc was selected as the solvent for producing the thin films. The solvent was procured from Sigma-Aldrich (Merck SA) from their ReagentPlus range. All plasticizers used were procured from Sigma-Aldrich (Merck SA); purities are indicated in Table 1. All solvents and plasticizers were used as received without any extra purification.

TABLE 1 | Keywords awarded to each plasticizer to ease reporting.

Key	Chemical	Key	Chemical
P1	2,2,4-trimethyl-1,3-pentanediol dibenzoate	P4	Di(ethylene glycol) dibenzoate (96%)
P2	Di(propylene glycol) dibenzoate (75%)	P5	Benzyl butyl phthalate (98%)
P3	Dibutyl phthalate (99%)	P6	Glyceryl tribenzoate (95%)

To ease analysis and reporting, each plasticizer was designated a keyword as indicated below. Samples were named according to the weight percentage plasticizer and plasticizer key (e.g., 50P1 indicates 50 wt% plasticizer P1 (2,2,4-trimethyl-1,3-pentanediol dibenzoate) present in sample).

2.2 | Method

2.2.1 | Operating Conditions Determination

Initial exploratory experiments were performed in-house to determine the most important operating conditions, namely the solvent, solids concentration in solution, dissolution temperature, and drying temperature. These were all dependent on the specifications of the larger overarching project. The main aim of the overarching project was to produce a PVDF-based solution to be used as a UV-protective topcoat on PVC-coated polyester textiles applied via the dip-coating method. While the coating method dictated the solids concentration in solution due to the need for a particular viscosity, the degradation temperature of the base textile controlled the maximum drying temperature of the solution to create the thin film. The aim was to mimic the topcoat creation process as closely as possible.

Thermal gravimetric analysis (TGA) was used to determine the degradation temperature of the PVC-coated polyester textile. The results indicated that an absolute maximum drying temperature of 120°C could be used; however, for safety, a drying temperature of 100°C was selected.

Next, the recommended solvent and solids concentration was investigated. Our study investigates the dissolution and stability of PVDF at room temperature and evaluates the performance of the four most well-known PVDF solvents—dimethylacetamide (DMAc), dimethylformamide (DMF), *N*-methyl-2-pyrrolidone (NMP), and dimethyl sulfoxide (DMSO)—across various PVDF concentrations (5, 10, 15, 20, 25, and 30 wt%).

The results showed that an absolute maximum of 20 wt% solids is recommended. However, 10 wt% was used in the current study. The results also showed, as can be seen in Figure 1, that DMAc was the only solvent that produced the clearest solution

over the widest range of concentrations. The discoloration of the final solution was not just affected by solid concentration but also by dissolution temperature. As shown in Figure 2, the DMAc solution did not discolor with an increase in dissolution temperature. A dissolution temperature of 50°C was selected to make the system more energy-efficient and to minimize solvent evaporation during dissolution.

2.2.2 | Plasticized Thin Film Production

The plasticizer thin films were produced by dissolving the PVDF powder in a beaker using DMAc as a solvent. The dissolution temperature was kept constant at 50°C by submerging the beaker in a silicon oil bath. The solution was stirred continuously using a mechanical stirrer. After the dissolution of the PVDF (approximately an hour of dissolution time), an equal amount of plasticizer (weight-based with regard to PVDF) was added. The stirring rate was increased slightly, and the solution was left for an hour to ensure homogeneity. Enough solvent was used to ensure a 90:10 weight percentage ratio between the solvent and solids (PVDF and plasticizer). Hence, in a sample denoted as 50P1, 50 wt% plasticizer P1 and 50 wt% PVDF were used, which forms part of the 10 wt% solids in the sample that was dissolved with 90 wt% DMAc.

Next, the solution was cooled to 25°C before casting the liquid onto a clean glass surface. The solution was spread evenly over the surface before drying at 100°C in a conventional convection oven for an hour. The samples were removed from the oven, left to cool, and submerged in warm water to remove the films from the glass surface. The same method was used to produce a

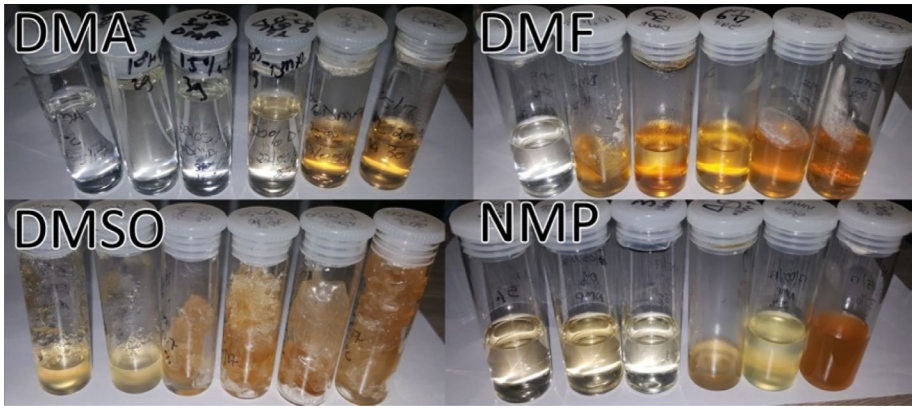

FIGURE 1 | Samples of the PVDF solution for each solvent taken at 25°C. For each solvent, the PVDF concentration increases from left to right, starting with a 5 wt% PVDF solution on the left and ending with a 30 wt% PVDF solution on the right, in increments of 5 wt% PVDF. [Color figure can be viewed at wileyonlinelibrary.com]

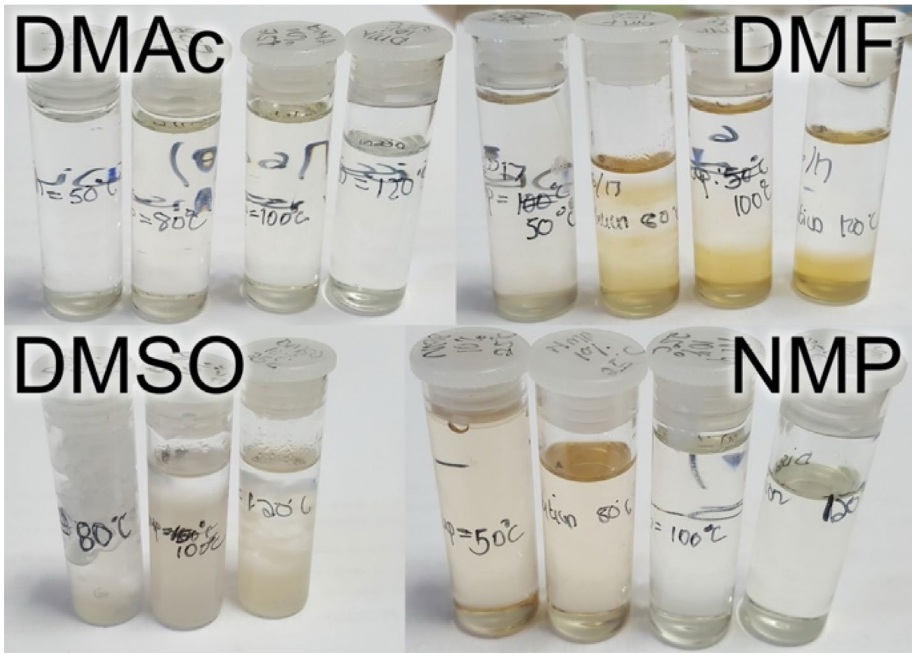

FIGURE 2 | Samples of PVDF solution for each solvent taken at 25°C. For each solvent, the dissolution temperature increased from left to right, starting at 50°C, 80°C, 100°C, and 120°C, except for the DMSO solvent, as PVDF did not dissolve at 50°C. [Color figure can be viewed at wileyonlinelibrary.com]

pure PVDF thin film as a reference. The raw PVDF powder data are denoted as PVDFraw and the film created as a reference as PVDFFilm.

To eliminate the effects of random variables that could influence the results, all processing parameters were kept strictly constant, including dissolution time and temperature, casting temperature, casting substrate, and drying temperature and duration. A drying temperature of 100°C—higher than the dissolution temperature of 50°C—was selected to negate any effects that the thermal history of the samples might have on the outcomes. For a fair comparison among different samples, equal weights of PVDF and plasticizer were used in this initial investigation.

2.3 | Characterization Methods

2.3.1 | FTIR: Spectral Analysis Method and PVDF Crystal Phase Determination

FTIR spectra were generated using PerkinElmer Spectrum Timebase software on a PerkinElmer Spectrum 100 with a Universal ATR Sampling Accessory installed. The instrument resolution was set at $4\,cm^{-1}$ with a data interval of $1\,cm^{-1}$. The wave number range studied was $4000–550\,cm^{-1}$. The force gauge on the ATR accessory was kept at 100 for all the samples while performing 32 scans per sample to ensure accuracy. The average thickness of the thin films were $5 \pm 0.025\,mm$.

The generated spectra were smoothed, and the baseline was corrected utilizing the asymmetric least squares method proposed by [15]. Reference spectra for all raw materials were collected in-house. Beer's Law, also known as the Beer–Lambert Law, was used to separate the thin film spectrum into the pure spectra of PVDF and the relevant plasticizer. Beer's law states that there is a linear relationship between the concentration and the absorbance of the solution, which enables the concentration of a solution to be calculated by measuring its absorbance, given that the molar absorptivity is known [16]. The law is mathematically expressed as:

$$A = \varepsilon \cdot c \cdot \ell \tag{1}$$

where A = absorbance (no units), ε = molar absorptivity ($L(mol\,cm)^{-1}$), c = concentration of the solution ($mol\,L^{-1}$), and ℓ = path length of the sample (cm).

However, Beer's law can also be applied to deconvolute the FTIR spectra of mixtures. For a mixture of two or more substances, provided that no chemical reaction takes place, the total absorbance at a particular wave number is the sum of the absorbances of each individual component. This can be expressed as:

$$A_{\text{Total}} = A_1 + A_2 + \ldots A_n \tag{2}$$

Assuming a two-component system, if the reference pure spectrum of each component is known, and a characteristic peak of one of the components (e.g., Component A) can be identified that does not overlap with that of Component B, the mixture spectrum can be deconvoluted. The reference spectrum of Component A is normalized so that the absorbance of the identified characteristic peak is equal to that of the same peak in the mixture spectrum. The reference spectrum of Component A can hence be subtracted from the mixture spectrum to produce the spectrum of Component B. This process can be applied to multicomponent systems; however, it does require.

In this instance, since PVDF can present in three main different crystal conformations, the reference FTIR spectrum of the plasticizer was subtracted using the method described to produce the "pure" PVDF spectrum. The deconvoluted PVDF spectrum was analyzed to determine the crystal phase structure composition of the thin film following the appropriate methods described in [17, 18].

2.3.2 | DSC Analysis: PVDF Degree of Crystallinity, Melting and Crystallization Temperature Determination

A PerkinElmer DSC 4000 was used in combination with Pyris software for data analysis. Thermal curves were obtained in a N_2 atmosphere by heating the sample from 30°C to 250°C at a rate of $10°C\,min^{-1}$, while crystallization curves were obtained by cooling the sample at the same rate from 250°C back down to 30°C. The subsequent repetition of the same cycle allowed to assess the corresponding melting characteristics of the samples crystallized in a controlled manner, providing some insight into the properties of these thin films if they were annealed under controlled conditions.

The degree of crystallinity (X_C) of the thin films was determined using Equation (3) as given in [19] which is the same as the equation used in [20, 21].

$$X_c = \frac{\Delta H_m / \varphi}{\Delta H_o} \times 100 \tag{3}$$

where φ is the weight fraction PVDF in the blend, ΔH_m is the melting enthalpy measured, and ΔH_o is the melting enthalpy of PVDF at 100% crystallinity. The value of ΔH_o is $104.5\,kJ\,kg^{-1}$ [22].

2.3.3 | Dynamic Mechanical Thermal Analysis (DMTA): Determination of the Glass Transition Temperature

The thin film glass transition temperature was determined using a PerkinElmer DMA8000. The sample was placed in a PerkinElmer material pocket and subjected to a single cantilever multifrequency (1 and 10 Hz) displacement of 0.05 mm over a temperature range of −150°C to 100°C achieved using liquid nitrogen. The average of three samples was used to determine the average glass transition temperature.

2.3.4 | SEM Analysis: Thin Film Surface Morphology

The surface morphology of the thin films was examined using one of two instruments depending on availability: the Zeiss Crossbeam 540 FEG SEM or the Zeiss Ultra PLUS FEG SEM. All the samples were prepared for analysis by coating the

surface with a thin layer of carbon in a Quorum Q150T Plus coating unit.

3 | Results and Discussion

3.1 | FTIR Analysis: PVDF Thin Film Crystal Phase

The thermal history of a thin film affects the phase conformation significantly [23]. Dissolution occurred at 50°C. However, drying occurred at 100°C, which is high enough to override the effects of the dissolution temperature. Based on the literature [23, 24], at a drying temperature of 100°C, a mixture of the polar and nonpolar phases should be observed with the nonpolar phases (α-phase) dominating.

Figure 3 compares the reference PVDF thin film created (PVDFFilm) with the unprocessed raw powder (PVDFraw). PVDFraw has very pronounced peaks at 763 and 614 cm^{-1} characteristic of the α-phase. The absence of any characteristic β-phase (1275, 840, and 1431 cm^{-1} [18]) and γ-phase (1234, 833, and 1429 cm^{-1} [18]) peaks in the PVDFraw spectrum confirms that the powder consisted exclusively of the high bonding energy α-phase.

The PVDFFilm consisted predominantly of the α-phase. However, a trace amount of the polar β-phase is also present, evident by the very small peak at 1275 cm^{-1} and a much more pronounced peak at 840 cm^{-1}. Interestingly, there is a possibility that a minute amount of γ-phase is also present, evidenced by the barely noticeable peak at 1234 cm^{-1} and a small peak at 833 cm^{-1}. However, this peak is so small that it can be considered negligible.

Figure 4 compares the plasticized films directly after production with that of the pure PVDF film. The characteristic peaks of plasticizers P1–P5 can be observed around the wave number 1716 cm^{-1}. The presence of this peak in the FTIR spectrum of samples 50P1–50P5 confirms that the drying process did not remove any of the plasticizer. It is quite evident that the characteristic peak of sample 50P6 is quite different from the other plasticizers and can be seen at wave numbers 1773 and 1799 cm^{-1}. Comparing the characteristic peaks of each of the plasticizers with the FTIR spectrum of pure PVDF, it is evident that they can

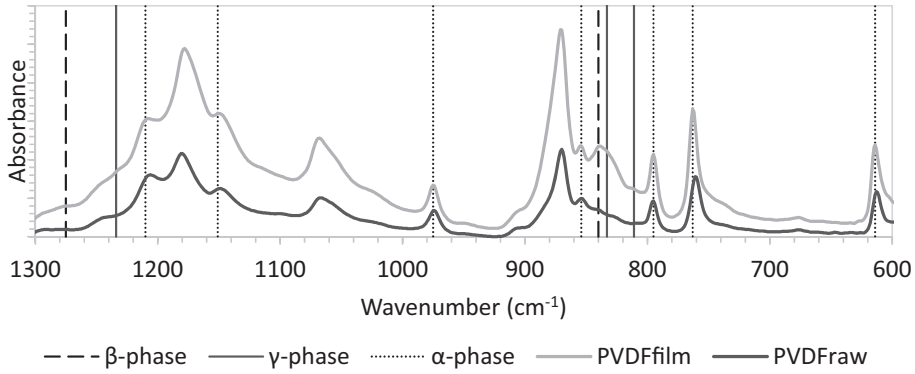

FIGURE 3 | The reference spectra from the virgin PVDF powder and the reference PVDF thin film.

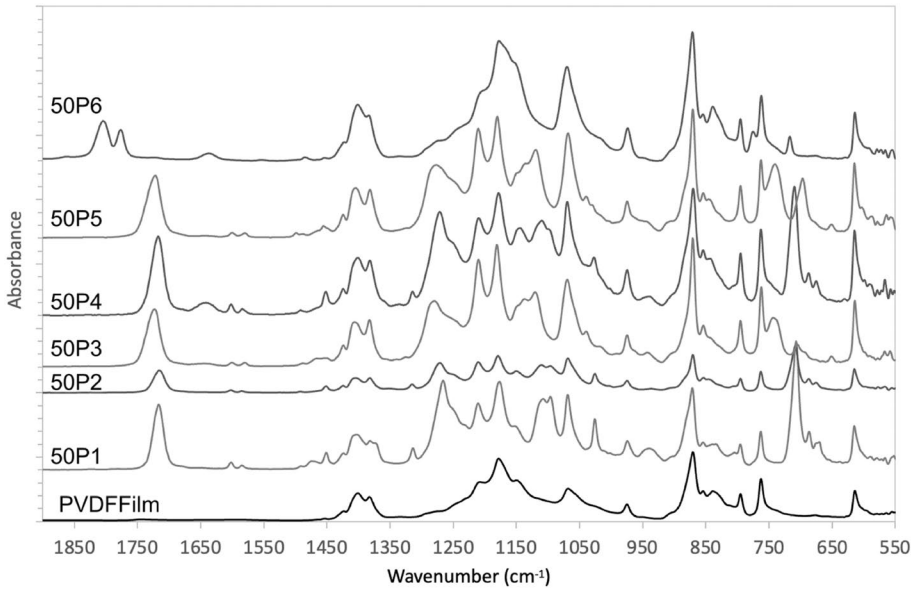

FIGURE 4 | The non-deconvoluted FTIR spectra of the plasticized thin films in comparison with the reference PVDF thin film (PVDFFilm). The characteristic peaks of plasticizers P1–P5 can be observed around wave number 1716 cm^{-1}.

be used following Beer's law to deconvolute the mixture spectrum, as PVDF has no peaks at these wave numbers. This process was used to produce the FTIR spectra displayed in Figure 5.

Analysis of the fully deconvoluted FTIR spectra of the plasticized thin films was performed in comparison with that of the PVDF reference thin film (PVDFFilm). All the plasticized thin films contained very strong absorption bands characteristic of the α-phase (763 and 614 cm^{-1} [18]) as shown in Figure 5.

Following the method outlined in [18], the spectra in Figure 6 were first inspected for the characteristic peaks of the β- and γ-phases at 1275 and 1234 cm^{-1}, respectively. Sample 50P2 exhibited a significant peak at 1275 cm^{-1}, which was considerably larger than that observed in the reference film (PVDFFilm). All the other samples displayed a peak at a similar wave number; however, this peak was notably shifted. This shift may be an artifact resulting from the removal of the plasticizer spectrum using Beer's law. Comparing the pure PVDF spectrum in Figure 4 with the other non-deconvoluted spectra, it is evident that the additional peaks in this area are due to the incorporation of the plasticizer. Hence, it stands to reason that during the deconvolution process, some subtraction error may leave behind certain artifacts. Such artifacts could distort the data obtained in identifying both the β- and γ-phases. Nonetheless, these are not the only characteristic FTIR peaks analyzed to ascertain the presence of these phases. As noted in [17], the final phase conformation of PVDF can only be confirmed

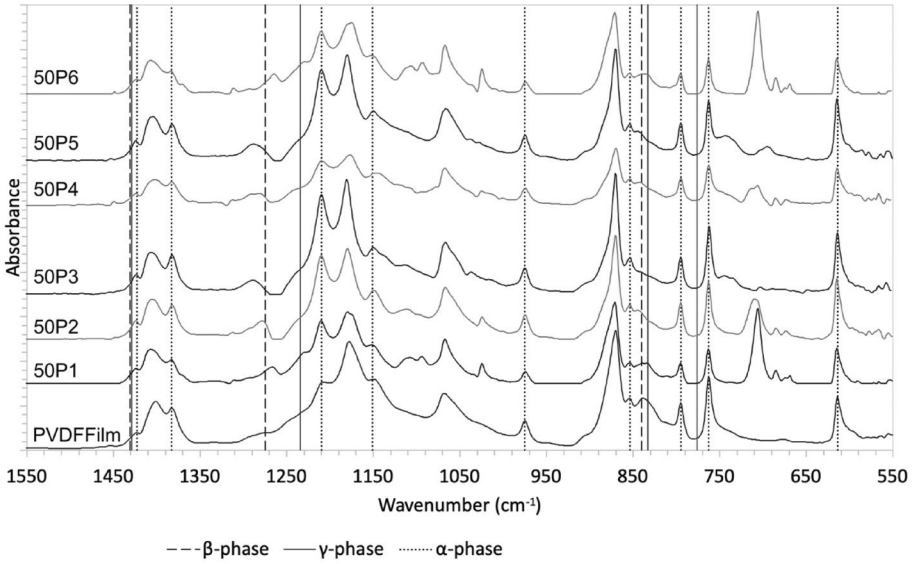

FIGURE 5 | The deconvoluted FTIR spectra of the plasticized thin films in comparison with the reference PVDF thin film (PVDFFilm) produced over the wave number range indicate the characteristic PVDF phase bands.

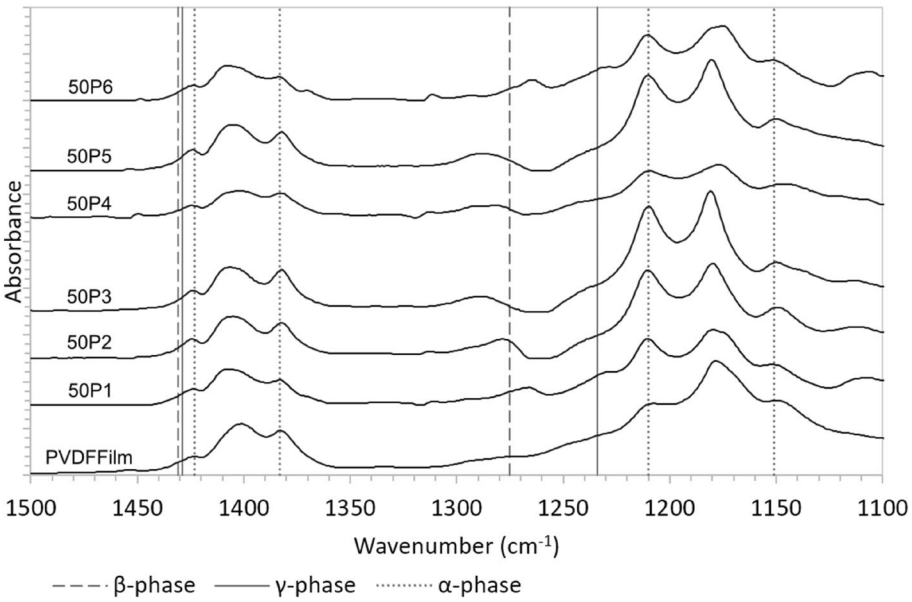

FIGURE 6 | The partial FTIR spectra, over the range 1100–1500 cm^{-1}, of the plasticized thin films in comparison with the reference film over the wave numbers that contain the main characteristic α-, β-, and γ-phase bands as suggested by [18].

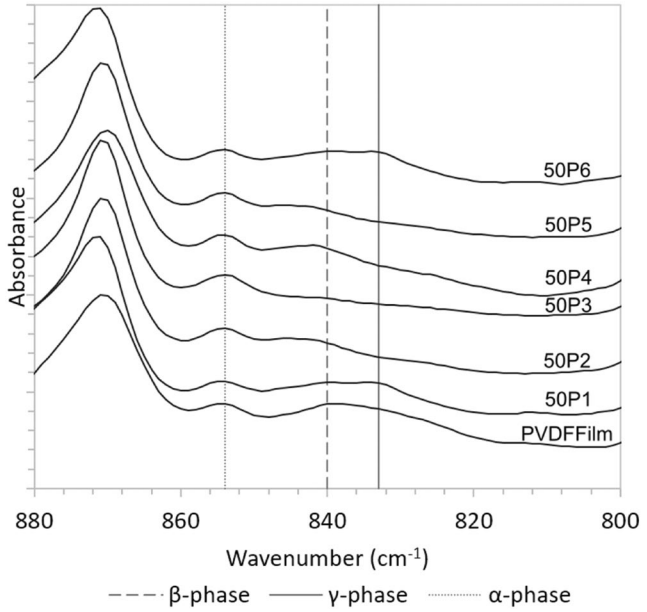

FIGURE 7 | The partial FTIR spectra, over the range 800–880 cm^{-1}, of the plasticized thin films in comparison with the reference film over the wave numbers that contain the main characteristic α-, β-, and γ-phase bands.

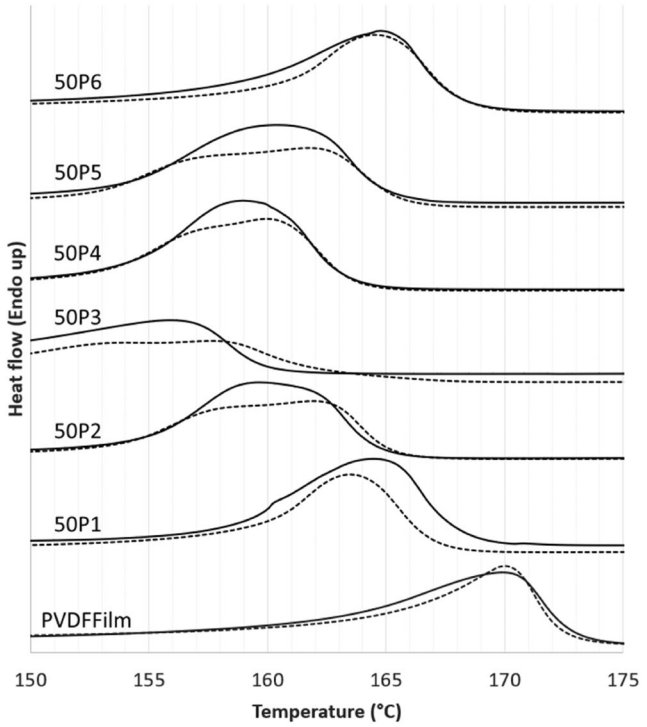

FIGURE 8 | Plasticized PVDF films melting DSC thermograms compared with a virgin PVDF film made under the same conditions for the initial (—) heating cycle and secondary (--) heating cycle. The secondary heating cycle represents the properties of the films being annealed under controlled conditions.

through a secondary analysis technique. FTIR analysis can provide guidance on what to scrutinize while verifying with a secondary analysis method, which in this instance was DSC. Samples 50P1 and 50P6 were the only samples that exhibited any significant peak around 1234 cm^{-1}, suggesting the potential presence of the γ-phase.

Closer inspection of the spectra over the range 880–800 cm^{-1} (Figure 7) suggests the presence of the β-phase with a defined peak at 840 cm^{-1} for the PVDFFilm and samples 50P1 and 50P6. Similarly, samples 50P6 and 50P1 both have peaks at 833 cm^{-1}, strengthening the possibility of the presence of the γ-phase. A slightly shifted peak is present in samples 50P2, 50P4, and 50P5 around 842 cm^{-1}, which might hint at the presence of the β-phase. Based on the FTIR analysis, plasticizers P1 and P6 had the most noticeable effect on the crystal phase, with both the β- and γ-phase being present. Plasticizers P2 and P4 increased the formation of only the β-phase, whereas P3 and P5 had no significant impact on the phase conformation other than decreasing the β-phase, as was evident in the reference film.

The above results all point to the possible inclusion of very small molar amounts of the β- and γ-phases based on the relative peak heights compared to the characteristic peaks of the α-phase. Referring back to Beer's law and Equation (1), there is a direct linear relationship between the peak absorption height and the concentration. In comparison, the height of the characteristic peaks of the α-phase in all of the produced samples is much larger compared to that of the β- and γ-phases. This concludes that the amount of β- and γ-phase content in the samples could be considered negligible when considering their overall contribution to the properties of the overall sample properties. This finding is in line with that proposed by several authors [18, 25–28] but particularly that of [23, 24]. At a drying temperature of 100°C, the polarity of both the solvent and plasticizer no longer influences the phase formation.

3.2 | DSC and SEM Analysis

DSC is a technique commonly used to determine or confirm not only the PVDF phase conformation but also the polymer crystallinity. In this study, DSC was primarily used to determine the viability of the additives as a plasticizer by investigating phase separation. Secondly, the analysis technique was used to determine the effect of the plasticizer on PVDF's crystallinity and to investigate or confirm PVDF phase conformation.

PVDF crystalline phases in the films need to be considered in the analysis of the thermograms as different phases have different melting peaks. The melting temperature (T_m) of the various phases is influenced by several factors, including the polymer's molecular weight, polymerization conditions, thermal history of the film, and morphological characteristics such as polymer defects and crystalline size [29–32]. However, since it was confirmed via FTIR analysis that the samples are predominantly composed of the α-phase, there is no need to be concerned about the effect of different phase melting points.

Figure 8 shows the thermograms of all the plasticized films compared to that of the pure PVDF reference film. It also shows the endotherms for the second DSC run used to simulate the annealing of the films under controlled conditions. The first reference PVDF film melting endotherm is broad with a peak at 170°C. FTIR analysis showed that the film consisted predominantly

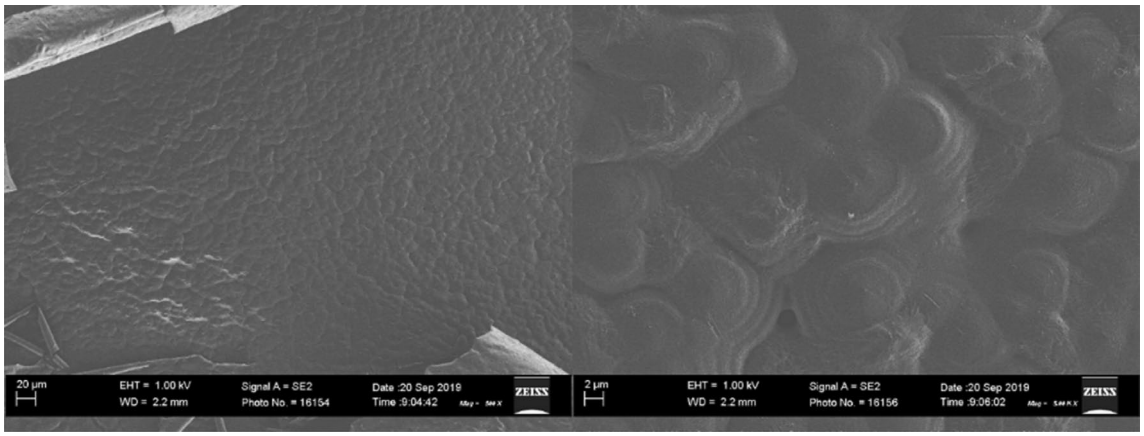

FIGURE 9 | SEM analysis of the pure PVDF film. Magnification of the image on the left is 500 and 5000 on the right. The unit scale of the left is 20 and 2 μm on the right.

of α-phase with a minuscule presence of β-phase. Hence, the α-phase melting temperature for the PVDF used is 170°C. The peak is quite broad, which could be due to the slight variation in spherulite sizes seen in Figure 9.

The PVDF melting peak becomes sharper when annealed above the melting temperature. Annealing at these conditions provides the polymer chains with sufficient energy to reorient and pack more efficiently into uniform well-defined crystalline regions, resulting in more perfect crystals that have a narrower melting transition. The peak temperature stays the same, confirming that the predominant crystalline α-phase remains. Several authors showed that films annealed or crystallized at temperatures higher than 160°C for short periods of time consisted of pure α-phase [25, 27, 30, 33]. Samples typically need to be held at very high temperatures for much longer periods (typically hours) to achieve α- to γ-phase transformation [31, 34].

It is clear from the thermograms of the plasticized films that the plasticizers caused a significant reduction in the film melting temperature. FTIR analysis confirmed that these films consisted predominantly of the α-phase, hence, the reduction in melting temperature is not due to a change in phase conformation but is attributed purely to the plasticizer.

The melting peaks of all the plasticized films were remarkably broader than those of the reference film. The broadened melting curves suggest a reduction in crystal perfection, a greater variation in crystal sizes, or a combination of both effects.

This broadening could be explained by the fact that during the melting process, the plasticizer is typically expelled from the crystalline regions and accumulates in the amorphous areas. This expulsion broadens the melting temperature range and lowers the melting point due to the increased free energy in the amorphous phase [35]. This migration of the plasticizer could cause momentary heterogeneous distributions of the plasticizer throughout the film, causing varying melting behavior to occur. This migration is a normal phenomenon that can occur during the melting stage. Once the mixture is cooled from the melt, the plasticizer reintegrates into the crystalline phase of the polymer, creating a more heterogeneous distribution. Hence, it does not affect the overall mechanical properties of the film after cooling. This is confirmed when considering the secondary melting curve, where a relatively similar melting temperature profile is observed, confirming that the material properties have not changed significantly.

As illustrated in Figure 10, the presence of a plasticizer induces the formation of substantially larger and more varied crystals, which could also explain the broadening of the melting curve as each crystal may differ in perfection and size.

Polymer crystal growth is primarily influenced by two factors: the solvent evaporation rate and the nucleation rate. These factors are interrelated, but the solvent evaporation rate typically has a more dominant influence [36–40]. The addition of the plasticizer can influence both of these factors. In this case, it seems that the plasticizers decreased the nucleation density, leading to the formation of significantly larger crystal sizes compared to that of the reference PVDF film, where the average spherulite diameter was measured at 9.7 μm (see Figure 9).

Plasticizer P3 exhibited the most significant influence on the melting temperature, initiating the first melting transition at approximately 140°C and peaking at 154°C. The broad melting curve observed can be attributed not only to the plasticizer's impact but also to the formation of a wide range of spherulite sizes, spanning from 10 to 40 μm, as illustrated in Figure 10c.

The secondary melting curve remains broad, displaying a slight double endothermic peak. This shift in melting behavior may be associated with the formation of both α- and β-phase crystals under controlled annealing conditions. As depicted in Figure 11c, the annealing process led to the development of a bimodal spherulite size distribution, with spherulites averaging approximately 140 μm alongside smaller ones around 20 μm. The double endothermic peak is likely due to the melting of these differently sized crystals at distinct temperatures. As [23] explained, at elevated crystallization temperatures, the influence of solvent or plasticizer polarity on crystal formation diminishes, with the crystallization rate instead becoming the dominant factor.

The presence of P3 resulted in a porous film structure, suggesting immiscibility with PVDF or very high solvent evaporation

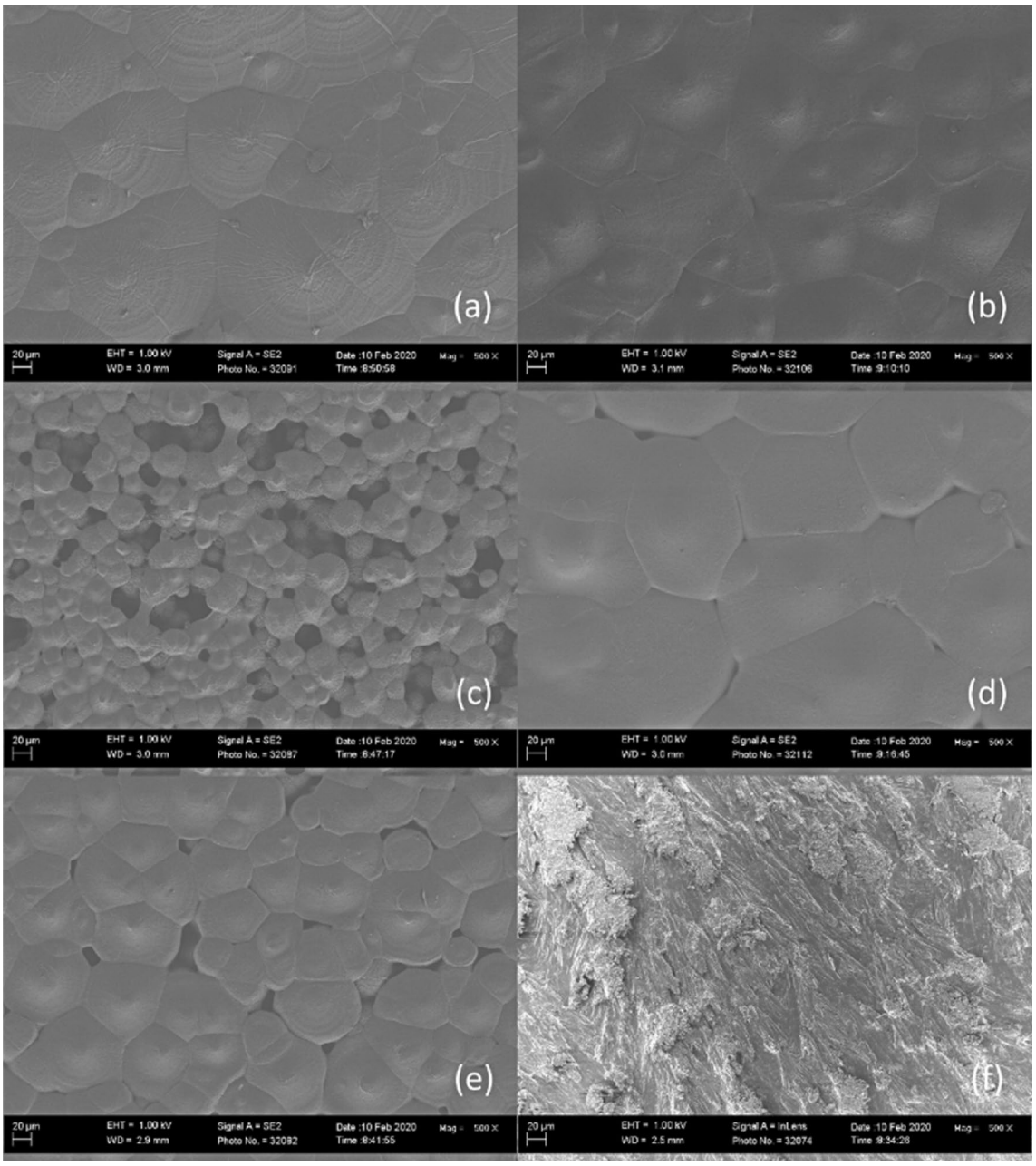

FIGURE 10 | Surface morphology images of the original six plasticized PVDF thin films. (a) 50P1, (b) 50P2, (c) 50P3, (d) 50P4, (e) 50P5, (f) 50P6. The unit of the scale indicated on the images is 20 μm. The images were obtained at a magnification of 500×.

rates. The increase in spherulite size after annealing under controlled conditions, where no solvent evaporation occurred, indicates that the plasticizer-solvent interaction had a significantly greater impact on spherulite formation during the initial thin film production process. This suggests that the addition of P3 not only significantly increased the solvent evaporation rate but also enhanced nucleation density, leading to the formation of a highly porous film.

The size and distribution of PVDF's spherulites significantly affect its mechanical integrity, flexibility, and overall barrier properties, particularly in the context of a protective topcoat. Large, unevenly distributed spherulites can create weak points, leading to cracks or voids where moisture, dirt, and UV radiation may penetrate. Consequently, although sample 50P3 contains small, relatively evenly distributed spherulites, the film's highly porous nature renders it unsuitable for use as a protective topcoat.

The DSC analysis of sample 50P1 revealed a slight shoulder peak at 160°C, with a primary melting temperature peaking at 164°C. This shoulder peak can be attributed to the presence of smaller crystals, approximately 20 μm in size, interspersed among much larger spherulites averaging 170 μm, as observed in Figure 10a. Although FTIR spectroscopy suggested the possible presence of a minor quantity of γ-phase crystals, this was not evident in the DSC melting curve. Annealing led to a slight reduction in the peak melting temperature, indicating an alteration in the crystalline structure.

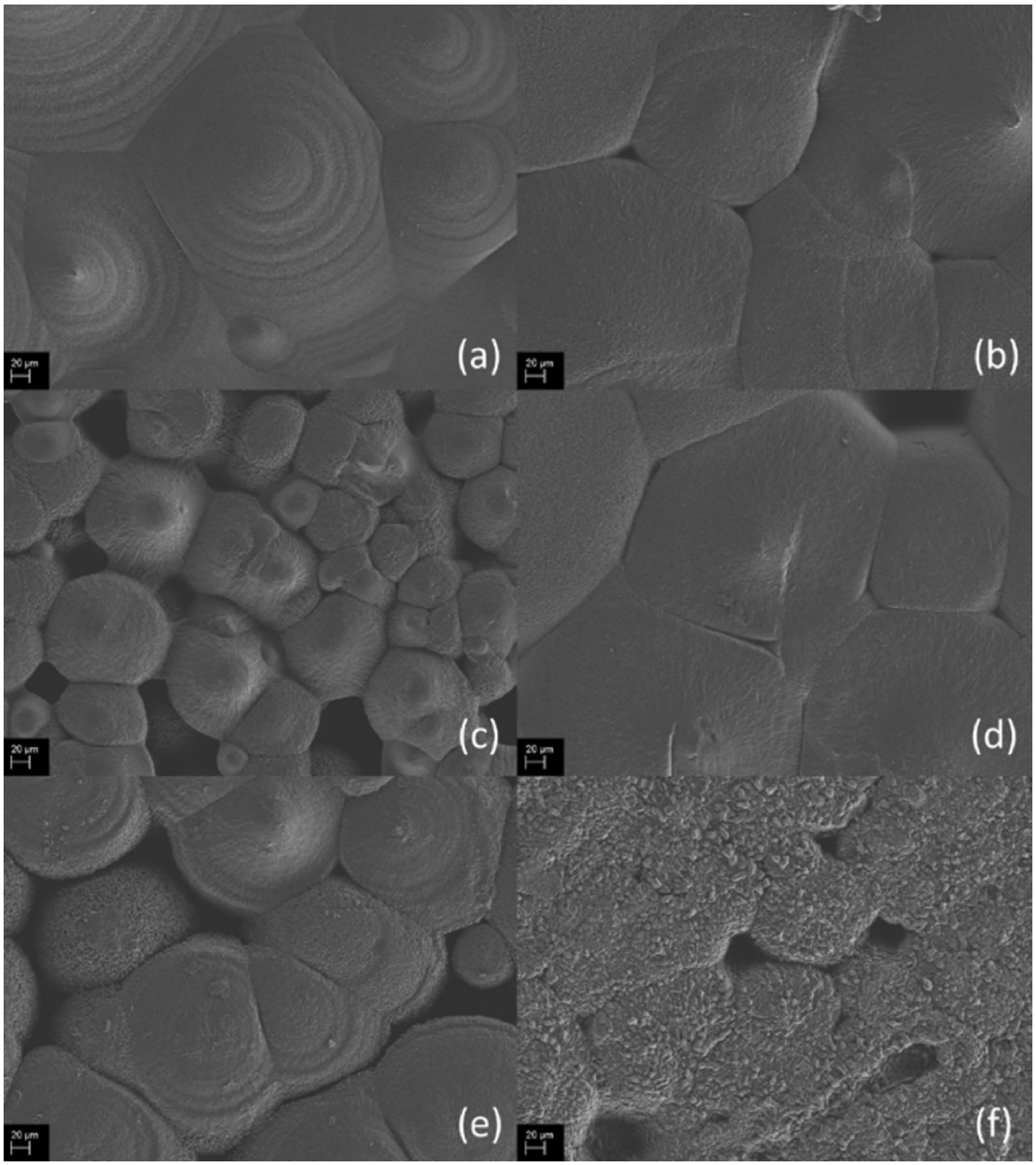

FIGURE 11 | Surface morphology images of the six plasticized PVDF thin films after the DSC annealing process. (a) 50P1, (b) 50P2, (c) 50P3, (d) 50P4, (e) 50P5, (f) 50P6. The unit of the scale indicated on the images is 20 μm. The images were obtained at a magnification of 500.

Post-annealing, SEM images (Figure 11a) showed a formation of larger, more uniform spherulites. Although some smaller spherulites persisted, the overall uniformity of the melting curve suggests their impact was negligible. This uniformity and the absence of porosity, cracks, or voids indicate that plasticizer P1 achieved a more homogeneous distribution throughout the film after annealing, signifying good miscibility with PVDF at the current concentration.

Interestingly, sample 50P1 is the only sample that led to the formation of distinct ringed spherulites. All the other samples, except 50P5 and 50P6, exhibit spherulites with radial lamellae that extend from a defined central point. The spherulites in sample 50P5 appear to include a mixture of both types of spherulites. Several authors in the literature [25, 26, 29, 34, 41–43] have made mention of the different types of spherulites.

Gregorio and Cestari [25] identified three spherulite types: ringed, non-ringed, and mixed, suggesting that spherulite form depends on the crystallization temperature. Ringed spherulites have lower nucleation and growth rates than non-ringed ones. Later, Gregorio and Capitao [41] found that ringed spherulites form exclusively from the α-phase at crystallization temperatures below 155°C, while non-ringed spherulites are predominantly of the γ-phase above this temperature. Their study, which analyzed films at various crystallization temperatures for extended periods, revealed that ringed spherulites can consist of both α- and γ-phases, depending on temperature and time. FTIR

analysis of the plasticized films in this study revealed that they consist predominantly of the α-phase which, according to the literature, can take two forms: ringed and non-ringed with radial lamellae emanating from a central point. Hence, the results seen in Figures 10 and 11 reinforce that the films consist of the α-phase even after annealing. The reasoning behind the formation of the different versions of α spherulites has not been explained in the literature. It might be that the ringed spherulites are more structured and might melt at a slightly higher temperature than non-ringed ones.

The melting endotherm of sample 50P2 is broader than that of sample 50P1 but less broad than that of sample 50P3. Figure 10b illustrates the crystals produced during solution casting. The incorporation of plasticizer P2 resulted in a narrower distribution of crystal sizes within the polymer matrix, with small crystals measuring at least 50 μm and large crystals up to 120 μm. This suggests that P2 achieved a more homogeneous dispersion throughout the polymer.

After annealing the film, much larger spherulites are formed, which could explain the slight increase in melting temperature observed on the secondary endotherm curve. The slight double endotherm peak is attributed to the formation of a much larger variation in crystal sizes (Figure 11b) compared to the original as-cast film. The original film exhibited no signs of voids or porosity, indicating that P2 is miscible with PVDF under solution casting conditions. However, after annealing, clear signs of voids and spherulite separation suggest that the plasticizer becomes less miscible. The miscibility between PVDF and the plasticizer can decrease at elevated temperatures, leading to phase separation during annealing. Phase separation creates regions rich in PVDF and regions rich in plasticizer, resulting in voids and structural discontinuities upon cooling.

Plasticizer P4 (Figure 10d) caused the formation of much larger spherulites than that of P5 (Figure 10e); however, 50P4 had a lower peak melting temperature. The difference in melting temperatures is explained by the effect of the plasticizer and the crystal perfection. Additionally, both samples show a slight double endotherm curve after annealing. The difference in the two peaks of 50P5 is more pronounced due to the inclusion of very small spherulites, as seen in Figure 11e, whereas, 50P4 contains a more even distribution of large spherulite sizes (Figure 11d). Voids and separation of spherulites are present in both sample films before and after annealing. These are less pronounced in sample 50P4 than in samples 50P3 and 50P5, implying that P4 might be a bit more compatible with PVDF than P5. After annealing, the voids and spherulite separation become more pronounced in sample 50P5. The surface of the P4 spherulites is smoother and less porous than that of the P5 spherulite before and after annealing. Before annealing, the spherulites of 50P5 are more connected, whereas annealing caused the formation of conglomerates of spherulites, solidifying the fact that P5 might not be miscible with PVDF under the current concentrations.

Interestingly, FTIR analysis of sample 50P6 indicated the possible presence of the β-phase; however, the DSC endotherm did not corroborate this finding. This discrepancy may be due to the β-phase being present in such a small percentage that it had a negligible effect on the melting temperature of the film.

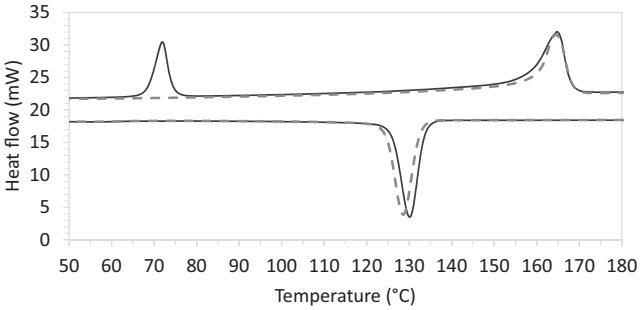

FIGURE 12 | Complete DSC thermal cycles for sample 50P6. The initial heating and cooling cycle is indicated with a solid line. The secondary heating cycle represents the properties of the films being annealed under controlled conditions.

Although a slight narrowing of the melting curve is observed after annealing, there is no change in the peak melting temperature. It is important to mention that during the initial DSC analysis, a sharp peak is seen around 73°C in Figure 12. This peak is due to the melting of plasticizer P6 crystals. P6 is the only solid plasticizer analyzed in the study. This peak is absent during the secondary analysis, indicating that the plasticizer required annealing to be incorporated fully into the PVDF polymer matrix. As seen in Figure 10f, plasticizer P6 is the only plasticizer that does not cause the formation of typical PVDF spherulites during solution casting. Slight spherulite formation can be seen after annealing (Figure 11f) above the melting temperature of PVDF. However, the surface of the film is not as smooth as the other films. A closer inspection of the film indicated the formation of different types of very small crystals seen in Figure 13. After annealing, the incorporation of P6 caused much larger and more defined crystals to form. This might be due to plasticizer P6 being a solid at room temperature. Curiously, the formation of different-sized, more defined crystals had a minor effect on the peak melting temperature with a downshift of only 1°C. Even though P6 caused the formation of very small crystals, the melting temperature was higher than plasticizers P2–5 before annealing and remained higher than all the plasticizers after annealing. After drying in the convection oven, a solid white brittle film was produced. It is clear that P6 is not a viable plasticizer of PVDF in the production of flexible protective topcoats for architectural textiles; hence, no further analyses were performed on samples 50P6.

Figure 14 shows that the plasticizers caused a decrease in the crystallization temperature. The largest decrease was seen in samples 50P2, 50P4, and 50P5. Since plasticizers reduce intermolecular forces and increase chain mobility, the PVDF chains remain mobile over a wider range of temperatures. This means that lower temperatures are required to initiate crystallization. Plasticizers also affect the thermodynamic balance between the amorphous and crystalline phases of the polymer. The free energy between these two phases is reduced, making it less favorable for crystallization to occur at higher temperatures. After annealing, the crystallization temperature of samples 50P2, 50P4, and 50P5 remained the same even though larger crystals were produced. Interestingly, samples 50P1 and 50P6 had similar crystallization temperatures before and after annealing. Sample 50P3's crystallization temperature curve is very broad similar to its melting temperature curve. This effect can be

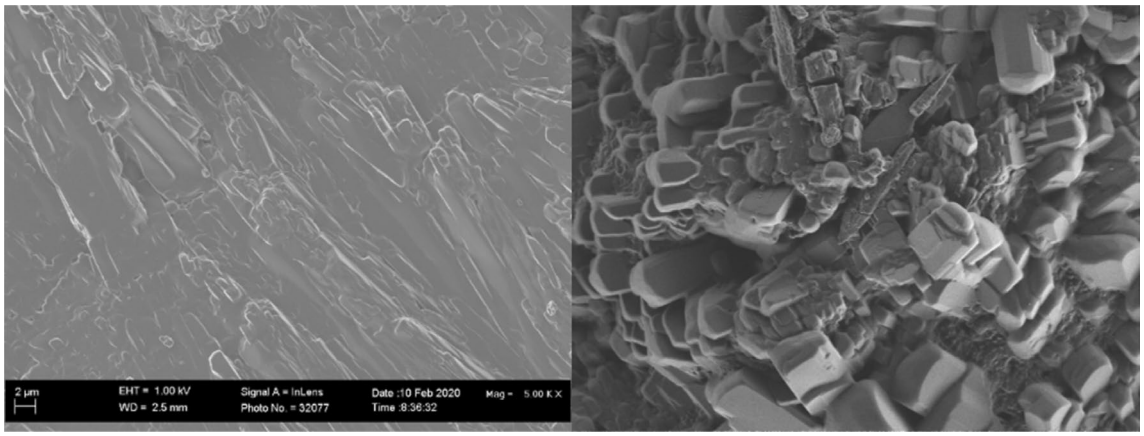

FIGURE 13 | A close-up of the films created using plasticizer P6 before (left) and after (right) DSC analysis. The film samples were magnified 5000 times. The scale on the images is 2 µm.

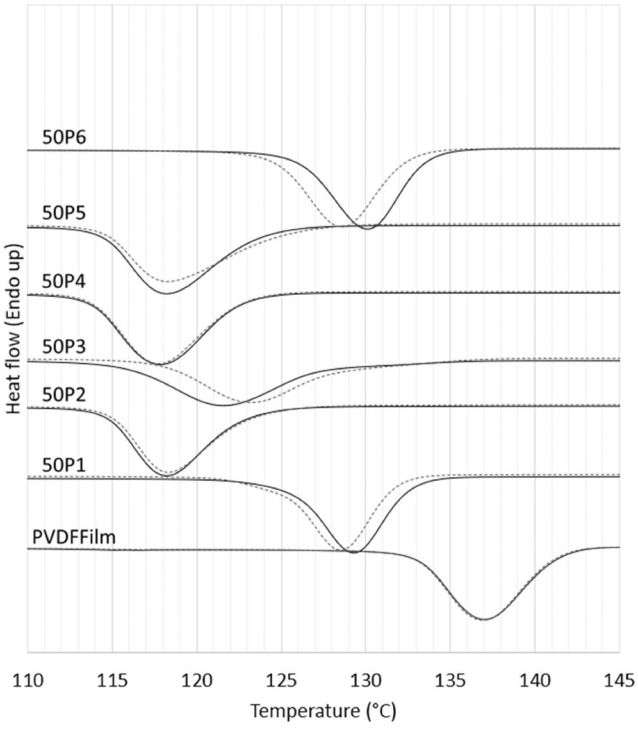

FIGURE 14 | Plasticized PVDF films crystallization DSC thermograms compared with a virgin PVDF film made under the same conditions for the initial (—) heating cycle and secondary (--) heating cycle. The secondary heating cycle represents the properties of the films being annealed under controlled conditions.

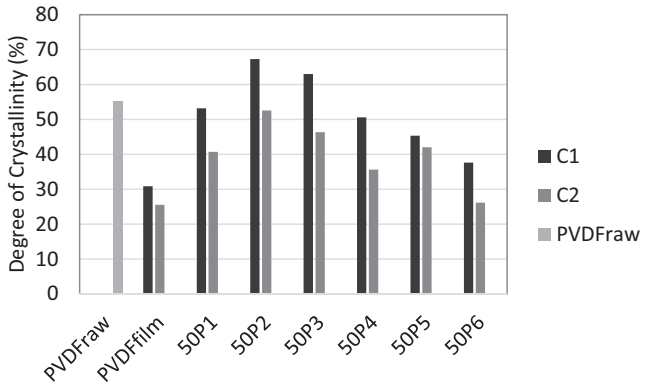

FIGURE 15 | A comparison of the degree of crystallinity for each plasticized PVDF thin film in relation to the reference film and the raw PVDF powder. C1 represents the first DSC thermal curve analysis, and C2 represents the second thermal curve analysis.

associated with the significant variation in crystal sizes formed during crystallization from the melt. The downward shift in crystallization temperature for samples 50P1 and 50P6 could indicate that the annealing process improved the incorporation of the plasticizer into the polymer matrix leading to a lower crystallization temperature.

The original pure PVDF powder had a much higher degree of crystallinity than the processed PVDF film created via solution casting (see Figure 15). During the solution casting process, the solvent interacts with the polymer molecules, disrupting orderly packing. Combining that with a relatively high evaporation rate, the polymer chains do not have enough time and mobility to rearrange into highly ordered crystals, lowering the degree of crystallinity. It is interesting to note that the degree of crystallinity of all the plasticized films is remarkably higher than the reference film, particularly in the case of sample 50P2. An increase in the degree of crystallinity was also noted by [11]. Typically, one would expect a plasticizer to lower the degree of crystallinity due to a disruption in the regular packing of the polymer chains. However, it seems in the case of PVDF the plasticizers could penetrate the molecular chains of both the amorphous and crystalline phases, generating more free volume and increasing the chain mobility of PVDF. This allowed the polymer chains to move more easily to align into ordered structures, leading to an increase in the degree of crystallinity. Plasticizers can also increase the crystallization rate and act as nucleating agents. Increased chain mobility alongside the increased crystallization rate, in this case, caused the formation of larger crystals than those in the reference film. After annealing, all the samples showed a reduction in the degree of crystallinity, with sample 50P5 experiencing the smallest decrease.

Typically, the addition of a plasticizer is expected to decrease the degree of crystallinity and reduce crystal sizes compared to the reference film. Due to this, a decrease in the heat of fusion and

TABLE 2 | The enthalpy of fusion and crystallization for all the samples. C1 represents the first DSC thermal curve analysis, and C2 represents the second thermal curve analysis.

Sample	Thermal curve number	ΔH_{fus} ($J g^{-1}$)	ΔH_C ($J g^{-1}$)
PVDFFilm	C1	32.25	43.51
	C2	26.66	40.71
50P1	C1	27.79	25.52
	C2	21.27	24.68
50P2	C1	35.15	31.15
	C2	27.47	30.82
50P3	C1	32.90	25.35
	C2	24.22	24.26
50P4	C1	26.43	28.55
	C2	18.62	28.89
50P5	C1	23.69	29.81
	C2	21.95	28.35
50P6	C1	19.66	23.81
	C2	13.66	24.02

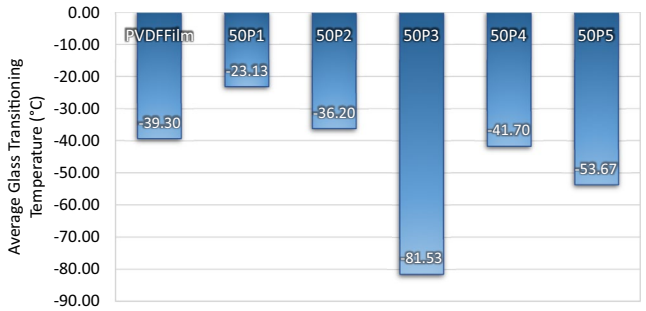

FIGURE 16 | The average glass transitioning temperature of the reference film in comparison to the plasticized films. The average of three samples was used to determine the average glass transitioning temperature of each film. [Color figure can be viewed at wileyonlinelibrary.com]

enthalpy of crystallization is expected. However, the current results show a contradiction: the degree of crystallinity in all plasticized films increased, and the crystals formed are much larger than those in the reference PVDF film. Despite this, there is still a reduction in both the heat of fusion and enthalpy of crystallization (Table 2). These contradictions could be explained by the crystals formed. Even though an increase in both the spherulite sizes and degree of crystallinity is observed, the presence of a plasticizer could disrupt the cohesive forces within the crystals during formation, leading to a high density of defects creating imperfect crystals. These imperfect crystals require less energy to melt, explaining the decrease in heat of fusion and the broadened melting curves.

In the case of PVDF, these plasticizers seem to increase the crystallization rate, most likely by affecting the solvent evaporation rate and chain mobility while decreasing the nucleation site distribution, causing the formation of much larger, less perfect crystals interspersed with the amorphous phase. Crystals with defects release less energy during crystallization, which explains the decrease in the enthalpy of crystallization.

Annealing caused a significant change in the enthalpy of crystallization; however, the heat of fusion decreased significantly after annealing, specifically in the case of samples 50P2–4. This decrease is directly linked to the decrease in crystallinity seen after annealing.

3.3 | DMTA Analysis: Thin Film Glass Transition Temperature (T_g)

All of the plasticized thin films were subjected to DMTA analysis except sample 50P6, as it was established as a nonviable plasticizer due to the formation of a brittle flaky thin film after solution casting. Figure 16 shows the effect of the different plasticizers on the T_g in comparison to the reference film.

Samples containing plasticizers P3–P5 exhibited a large decrease in T_g, with the 50P3 blend showing the most significant reduction. This lowering of T_g suggests enhanced polymer chain mobility and increased flexibility of the films, which is advantageous for coating applications. Even though Plasticizer P2 caused a significant reduction in the melting temperature (decreased by 10°C) and crystallization temperature (decreased by 19°C), the T_g increased slightly by 3°C. Sample 50P5's T_g decreased by 16°C, and 50P4's T_g decreased by only 4°C. From the T_g analysis alone, P3 looks like the most viable plasticizer. However, when selecting the most suitable plasticizer for a specific application, all factors that might influence its performance must be taken into account. In the current application—flexibilizing PVDF to produce a protective topcoat—both the surface morphology and the compatibility of the plasticizer with PVDF should be carefully evaluated alongside the T_g results. The reason for the differing effects of the different plasticizers in the T_g is discussed further in Section 3.3.1.

The surface of sample 50P3 (Figure 10c) was highly porous, possibly due to immiscibility with PVDF or an extremely high solvent evaporation rate. A film with this type of morphology will not offer any protection against UV; in fact, it could exacerbate the situation. Therefore, even though P3 significantly reduced the T_g, the surface morphology limits its viability. Nevertheless, it would be worthwhile to explore additional additives that could help modify the surface morphology, which is why P3 cannot be entirely dismissed.

A similar argument applies to samples 50P4 and 50P5 regarding their surface morphology, though the extent of the voids and porosity observed in these samples is not on par with that of sample 50P3. The surface of sample 50P4 bears some resemblance to that of sample 50P2 in terms of "smoothness," but not in spherulite size. However, the voids and somewhat disconnected nature of the spherulites in this sample present challenges for the requirements of a protective topcoat. It is essential to consider not just UV exposure but also other factors, such as moisture and

dirt, which could infiltrate the voids and cause the topcoat to begin separating.

Even though the T_g of sample 50P2 increased slightly, the thin film produced was remarkably more flexible than compared to a pure PVDF film of similar size and thickness. It is important to note that the exact mechanism of plasticization remains poorly understood, particularly in high molecular weight semi-crystalline polymers, such as PVDF, which can coexist in multiple crystal conformations. Several theories have been proposed to explain the mechanism of plasticization, notably the gel theory, the lubrication theory, and the free volume theory [8]. The gel theory posits that polymers form a three-dimensional network or gel, and plasticizers reduce the number of attachment points between polymer chains. By disrupting these connections, plasticizers enhance the flexibility of the polymer without compromising its structural integrity. The lubrication theory suggests that plasticizers act by reducing intermolecular friction, allowing polymer chains to slide over each other more easily; this theory underscores the importance of molecular polarity in selecting appropriate plasticizers based on the "like dissolves like" principle. Developed later, the free volume theory proposes that plasticizers increase the free volume within the polymer matrix, which lowers the glass transition temperature (T_g) and enhances flexibility by permitting greater mobility of polymer segments. Hence, even though T_g is used as a good indicator of the effectiveness of an additive's plasticizer ability, it should not be used as the only deciding factor.

Due to the semi-crystalline nature of PVDF, which often encompasses various polymorphic phases, it proves difficult to establish a singular, cohesive mechanism for plasticization. This challenge is further complicated by the lack of research into plasticization in PVDF under similar experimental conditions. The distinct amorphous and crystalline domains in PVDF create unique sites for plasticizer penetration. Moreover, existing theoretical models, such as free volume theory, lubrication theory, and gel theory [8], may either converge or differ in their explanations of the processes involved. Additionally, variations in the chemical structure of plasticizers and vital processing parameters—like solvent choice, evaporation rates, and annealing temperatures—add further complexity to plasticizers' dispersion and molecular interactions. While conventional characterization methods can detect bulk changes, such as alterations in melting and glass transition temperatures, these techniques lack the sensitivity to observe the transient, molecular-scale phenomena that ultimately govern plasticization. Therefore, establishing a singular, comprehensive mechanism remains an unresolved issue.

3.3.1 | Plasticizer Structural Analysis and Results Explanation

The effectiveness of a plasticizer in PVDF is significantly influenced by its molecular configuration and interactions with the PVDF polymer structure. The predominant crystal phase in this study, α-phase, features a nonpolar trans-gauche-trans-gauche′ (TGTG′) configuration (Figure 17). The —CH_2- and —CF_2— groups are oriented in alternating gauche and trans

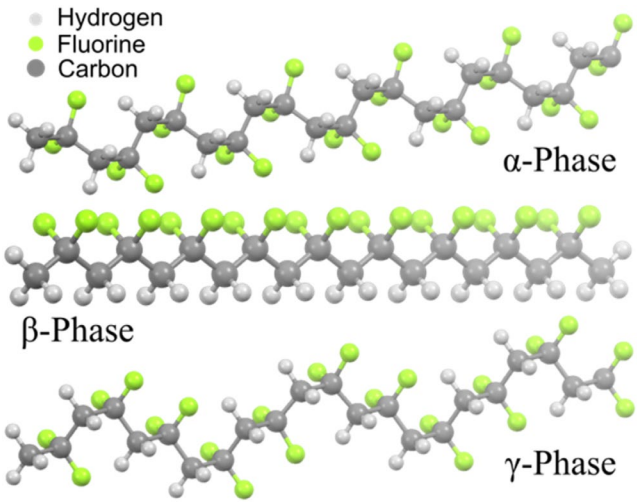

FIGURE 17 | The three main crystal structures of PVDF. [Color figure can be viewed at wileyonlinelibrary.com]

configurations along the chain, causing most of the dipoles to cancel each other out. This helical structure provides rotational flexibility along the polymer backbone and contributes to the material's overall flexibility.

Alternatively, in the functional groups of the β-phase (Figure 17), each —CH_2— and —CF_2— bond adopts a fully extended trans conformation along the polymer backbone. Because all the dipoles along the —CF_2— and —CH_2— units are aligned in the same direction, they add constructively, generating the highest net dipole moment. This phase is considered to be the most polar of all the main PVDF phases due to its piezoelectric functionalities.

The γ-phase is considered an intermediary phase between α- and β-phase, commonly described as "TTTG" or "TTTGTTTG," meaning mostly trans with occasional gauche linkages. While not as straightforwardly polar as the β-phase, the partially aligned dipoles in the γ-phase give it intermediate polar properties.

In α-phase PVDF, nonpolar chains pack closely together, stabilized mainly by London dispersion forces, which are the dominant but weaker intermolecular interactions compared to hydrogen bonds. Local dipoles from C—F bonds can induce dipoles in adjacent chains, slightly enhancing intermolecular attraction.

Based on these characteristics, an effective plasticizer should:

1. Be nonpolar or weakly polar to ensure compatibility and miscibility with the PVDF chains, based on Moorshead's empirical approach to plasticization [8].
2. Have a flexible molecular structure to enhance the rotational flexibility of PVDF chains and increase free volume within the polymer matrix, based on the free volume theory of plasticization.
3. Engage in van der Waals interactions, particularly London dispersion forces, to interact effectively with PVDF chains based on the lubrication theory.

4. Possess an appropriate molecular size—small enough to fit between polymer chains but large enough to disrupt their close packing, corresponding to the free volume theory.
5. Lack strong hydrogen bonding groups to prevent incompatibility or unwanted cross-linking with PVDF, as proposed by the gel theory.
6. Exhibit inductive effect capability to slightly enhance intermolecular attractions without overpowering existing forces, as described by Moorshead's empirical approach.

According to the free volume theory, an effective plasticizer significantly lowers the T_g of a polymer, thereby enhancing chain mobility within the polymer matrix. P3 exhibited a substantial decrease in the T_g of PVDF, indicating effective plasticization and increased chain mobility in the amorphous regions. The polar ester groups in P3 (Figure 18) interact with the polar C—F bonds of PVDF via dipole–dipole interactions, facilitating molecular-level miscibility. Plasticizer P3 is also the only plasticizer with only one benzene ring, which might contribute to the extreme effect that P3 has on the T_g compared to the other plasticizers. The bulkier nature of the benzyl groups in the other plasticizers introduces a higher level of steric hindrance, which may reduce their effectiveness. The decreases in crystallization and melting temperatures suggest that P3 disrupts the crystalline regions of PVDF, lowering the energy required for phase transitions. This disruption likely arises from the flexible alkyl chains of P3 interfering with the regular packing of PVDF chains. Despite interrupting crystalline regions, the significant increase in crystallinity and the formation of larger spherulites may indicate phase separation, where PVDF-rich regions crystallize more effectively while P3-rich regions remain amorphous. SEM results suggest that P3 acts as a nucleating agent for PVDF, facilitating the growth of spherulites. However, the formation of pores and voids supports the notion of limited miscibility and phase separation during solidification. The nonpolar alkyl chains of P3 reduce compatibility with highly polar PVDF, contributing to limited miscibility at higher concentrations. While dipole–dipole interactions lower T_g and enhance flexibility, the absence of hydrogen bonding and the presence of nonpolar segments limit the strength of these interactions, affecting the degree of miscibility. Reducing the concentration of P3 might improve film morphology while preserving plasticization.

P5 showed the second-largest effect on lowering the T_g of PVDF, suggesting it is a promising plasticizer. Similar to P3, P5's ester groups (Figure 19) interact with PVDF to increase chain mobility. P5 also has one alkyl chain similar to P3's two alkyl chains. The dipole–dipole interactions between the alkyl chain and PVDF might be why P5 showed the second-largest drop in T_g, as none of the other plasticizers has similar structures. The decrease in T_g implies partial miscibility with PVDF. However, the large increase in film crystallinity and formation of larger spherulites may indicate that P5 decreases nucleation sites, leading to less perfect crystals, especially considering the decrease in the heat of fusion. The voids and spherulite separation observed under SEM analysis indicate phase separation. The incompatibility with PVDF might stem from P5's larger molecular size due to an additional aromatic ring. The bulkier benzyl group increases steric hindrance, hindering uniform integration between PVDF chains and explaining the uneven distribution and phase separation. This rigidity also decreases flexibility, inhibiting effective interaction with PVDF chains and uniform disruption of intermolecular forces.

P4 exhibited a modest reduction in T_g, suggesting a limited enhancement of PVDF's chain mobility and flexibility. This small change implies that P4 does not significantly penetrate between PVDF chains or substantially reduce intermolecular forces. The decreases in melting and crystallization temperatures indicate that P4 interferes with the PVDF crystal lattice, though moderately. P4's relatively large size, due to two benzoyl groups (Figure 20) connected by a diethylene glycol moiety, introduces steric hindrance, making uniform integration between PVDF chains challenging. While P4 has high polarity from its ester groups and ether linkages—which can interact with PVDF's polar C—F bonds—the less polar, hydrophobic benzoyl groups reduce overall polarity. This combination leads to partial compatibility but not complete miscibility with PVDF. The presence of spherulite separation or voids suggests phase separation and limited miscibility at the current concentration.

P2 showed minimal change in T_g, indicating limited enhancement of chain mobility in the amorphous region and suggesting

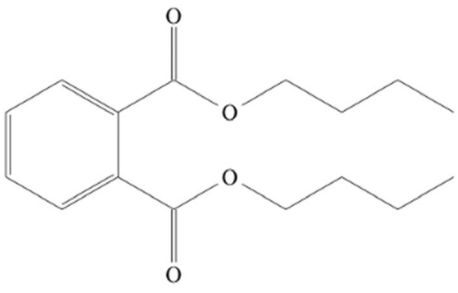

FIGURE 18 | Molecular structure of plasticizer P3.

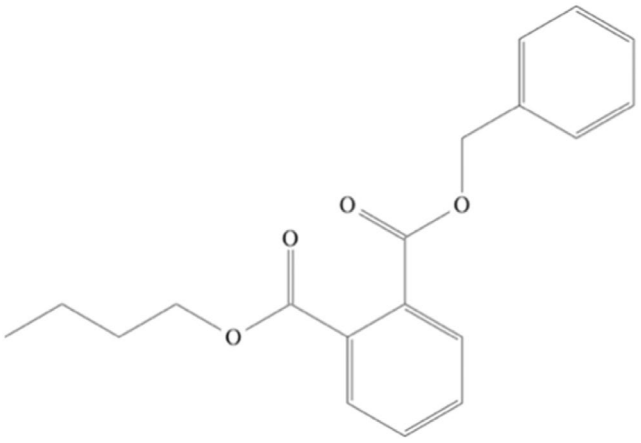

FIGURE 19 | Molecular structure of plasticizer P5.

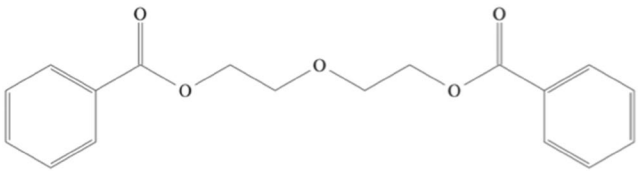

FIGURE 20 | Molecular structure of plasticizer P4.

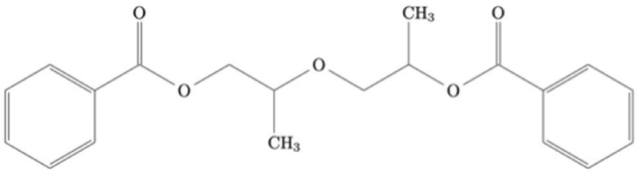

FIGURE 21 | Molecular structure of plasticizer P2.

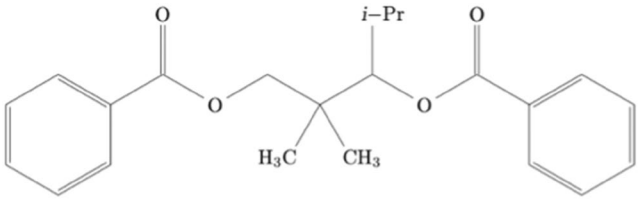

FIGURE 22 | Molecular structure of plasticizer P1.

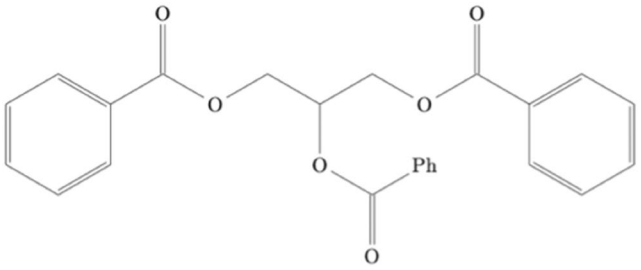

FIGURE 23 | Molecular structure of plasticizer P6.

limited miscibility there. However, changes in melting and crystallization temperatures suggest that P2 affects the crystalline phase of PVDF, indicating some level of miscibility. The significant increase in crystallinity and spherulite size demonstrates that P2 promotes PVDF crystallization, confirming miscibility with the crystalline region. The absence of voids and porosity suggests that P2 is well-dispersed within the PVDF matrix without phase separation, indicating good compatibility. Although similar in size to P5, P2 has higher flexibility due to ether linkages and propylene units (Figure 21), allowing it to conform to PVDF's chain structure and interact effectively. The combination of moderate molecular size, adequate polarity, and flexibility facilitates interaction with PVDF chains, promoting miscibility, especially in crystalline regions. Polar ester groups and ether linkages enable dipole–dipole interactions with PVDF's C—F bonds, while flexible aliphatic segments engage in van der Waals interactions, enhancing compatibility.

P1 caused an increase in T_g, indicating restricted mobility of polymer chains in the amorphous phase and suggesting anti-plasticization. This effect may render the material more brittle. A decrease in melting and crystallization temperatures shows partial miscibility with the crystalline phase, potentially acting as a nucleating agent and promoting larger crystal growth. The absence of voids or porosity indicates good dispersion without phase separation. P1's larger, less flexible, and bulky structure leads to steric hindrance, preventing easy integration between PVDF chains. Although polar ester groups can engage in dipole–dipole interactions with PVDF, these may not overcome steric hindrance and reduced polarity. P1 exhibits limited miscibility with PVDF, acting more as an anti-plasticizer in the amorphous phase and affecting the crystalline phase by promoting larger crystals. This limited miscibility suggests that P1 may not be ideal for applications requiring enhanced flexibility and toughness (Figure 22).

P6 was the least effective plasticizer. The T_g could not be measured due to the film's brittle nature, indicating that P6 does not enhance PVDF's flexibility. P6 does not act effectively in the amorphous regions, suggesting limited miscibility. Slight decreases in melting and crystallization temperatures indicate minimal effect on crystalline regions, and a slight increase in crystallinity suggests more crystalline region formation. The absence of spherulite formation and the presence of clumps indicate poor interaction with PVDF. The rough, brittle, and powdery film morphology points to significant phase separation and poor mechanical integrity. P6's large size and rigidity, due to bulky benzoyl groups (Figure 23), introduce steric hindrance, limiting integration between PVDF chains. Reduced polarity and rigidity hinder effective interactions, resulting in poor miscibility. While ester groups can engage in dipole–dipole interactions, steric hindrance and limited contact area weaken these interactions. Nonpolar benzoyl groups may only weakly interact via van der Waals forces, but the bulky structure limits effectiveness. Consequently, P6 leads to a brittle, nonuniform material with poor structural integrity and is unsuitable as a plasticizer for PVDF thin films requiring flexibility and uniformity.

The effectiveness of plasticizers in PVDF thin films is significantly influenced by molecular structure—particularly size, flexibility, and the balance between polar and nonpolar regions. Smaller or more flexible molecules (e.g., P3, P5) with appropriately positioned polar functionalities can disrupt the polymer's crystalline regions and reduce T_g, thereby enhancing chain mobility. However, excessive bulk or incompatible nonpolar segments can negate these benefits. For instance, P3 successfully lowers T_g and increases flexibility but exhibits limited miscibility at higher concentrations, leading to pores and phase separation. P5 similarly decreases T_g, but its larger aromatic ring introduces steric hindrance, resulting in phase separation and limiting uniform dispersion.

Plasticizers that are excessively large, rigid, or lack adequate polarity (e.g., P1, P6) may demonstrate negligible or even anti-plasticizing effects by raising T_g or producing brittle films. P1 increases T_g, restricting chain mobility in the amorphous regions, whereas P6 offers virtually no plasticization and leads to poor film integrity. P4 exhibits only a moderate reduction in T_g due to partial compatibility, limited by its bulky aromatic segments. In contrast, P2—although similar in size to P5—shows improved flexibility and polar interactions, aiding good dispersion and compatibility in the crystalline region. Overall, maintaining an optimal balance of molecular size, polarity, and flexibility is essential for achieving effective plasticization and consistent film morphology in PVDF systems.

4 | Summary and Conclusions

In this study, various plasticizers were examined to ascertain which would most effectively plasticize PVDF. The main

objective of this research was to identify the most suitable plasticizer that enhances the flexibility of PVDF-based thin films and yields a thin film with a surface morphology that serves as an acceptable protective UV-resistant topcoat for flexible architectural textiles.

Six different plasticizers were evaluated by producing PVDF thin films using the solution casting method. A 50:50 wt% solution of PVDF and each plasticizer was prepared in DMAc at 50°C. The resulting solution was cooled to room temperature, cast onto a clean glass substrate, and dried in a convection oven at 100°C. FTIR analysis confirmed that all films crystallized in the α-phase.

Plasticizers P1 and P6 performed the worst of all six plasticizers. P1 slightly lowered the melting temperature and showed no evident phase separation, showing partial miscibility with PVDF. However, it raised T_g, suggesting restricted chain mobility. Although it formed large spherulites and showed acceptable uniformity after annealing, its anti-plasticizing effect makes it not a viable PVDF plasticizer. P6, on the other hand, produced a very brittle, solid film with poor mechanical integrity, deeming it ineffective as a plasticizer.

Plasticizer P4 slightly reduced the *T*g, partially disrupting the crystallinity of PVDF, and modestly decreased the melting and crystallization temperatures. However, the presence of voids and somewhat disconnected spherulites highlights only partial compatibility, which poses potential issues for creating uniform protective coatings. It is advisable to explore other additives in the future to assess whether the surface morphology could be improved.

The two plasticizers that had the largest effect on T_g were P3 and P5, with P3 being the most significant. However, despite P3 exhibiting strong plasticizing action, significant porosity and limited miscibility were evident in the SEM images, rendering the film unsuitable as a protective topcoat without further modifications to address the porous structure. P5 increased spherulite size, suggesting a strong effect on chain mobility and crystallization. However, the bulkier molecule resulted in pronounced voids and spherulite separation, limiting uniform dispersion in PVDF and compromising its viability as a topcoat.

P2 reduced melting and crystallization temperatures, enhancing the degree of crystallinity and spherulite size. It blended well with PVDF, and no voids were detected via SEM analysis, indicating strong compatibility. Despite a slight increase in T_g, the film remained more flexible than pure PVDF, suggesting that it was effectively plasticized without compromising the film's integrity. Plasticizer P2 strikes the optimal balance between flexibility and compatibility, yielding a low-void film with suitable mechanical properties (due to an increase in crystallinity), making it the most viable plasticizer for creating flexible PVDF protective topcoats.

This simple method of producing a solution for dip coating makes this process easy to implement in underdeveloped areas without the need for expensive, sophisticated equipment. This will enable these regions to lengthen the lifespan of architectural textiles used as housing at a much cheaper rate.

Author Contributions

Anya Sonnendecker: data curation (lead), formal analysis (lead), investigation (lead), methodology (lead), project administration (lead), resources (lead), supervision (lead), writing – original draft (lead). **Matome W. Mametja:** data curation (supporting), formal analysis (supporting), investigation (supporting). **Johan Labuschagne:** funding acquisition (lead), project administration (equal), resources (supporting), supervision (supporting).

Acknowledgments

The study was financially supported by funding from the Fluorochemistry Expansion Initiative (FEI) that was managed by the South African Department of Science and Technology (DST) and from the Council for Scientific and Industrial Research (CSIR). The authors would like to thank Professor Philip Crouse who obtained the FEI funding for the project in its original form.

Conflicts of Interest

The authors declare no conflicts of interest.

Data Availability Statement

The data that support the findings of this study are available from the corresponding author upon reasonable request.

References

1. R. Dallaev, T. Pisarenko, D. Sobola, F. Orudzhev, S. Ramazanov, and T. Trčka, "Brief Review of PVDF Properties and Applications Potential," *Polymers* 14, no. 22 (2022): 4793, https://doi.org/10.3390/polym14224793.

2. A. Sonnendecker, D. Viljoen, B. Ameduri, and P. Crouse, "Chapter 10—Fluoropolymer-Based Architectural Textiles: Production, Processing, and Characterization," in *Fascinating Fluoropolymers and Their Applications*, ed. B. Ameduri and S. Fomin (Elsevier, 2020), 337–399, https://doi.org/10.1016/B978-0-12-821873-0.00010-2.

3. B. Ameduri and B. Boutevin, "Copolymerization of Fluorinated Monomers: Recent Developments and Future Trends," *Journal of Fluorine Chemistry* 104 (2000): 53–62, https://doi.org/10.1016/S0022-1139(00)00227-X.

4. B. Ameduri and B. Boutevin, "Synthesis, Properties and Applications of Fluoroalternated Copolymers," in *Well-Architectured Fluoropolymers: Synthesis, Properties and Applications*, 1st ed., ed. B. Ameduri and B. Boutevin (Elsevier Ltd, 2004), 187–230.

5. Lumiflon, "Formulating Highly Weatherable, Low VOC Liquid and Powder Coatings With FEVE Fluoropolymer Resin Technology," 2017.

6. B. Ameduri, "From Vinylidene Fluoride (VDF) to the Applications of VDF-Containing Polymers and Copolymers: Recent Developments and Future Trends," *Chemical Reviews* 109 (2009): 6632–6686, https://doi.org/10.1021/cr800187m.

7. S. B. Dibyendu, *Principles of Polymers: An Advanced Book* (Nova Science Publishers, 2013), 457–495.

8. A. Marcilla and M. Beltrán, "Mechanisms of Plasticizers Action," in *Handbook of Plasticizers*, 3rd ed., ed. G. Wypych (ChemTec Publishers, 2017), 119–134.

9. D. Chun-hui, W. Li-Guang, and X. You-yi, "Crystal Behaviour and Compatibility of PVDF-Plasticizer Blend System," *Journal of Functional Polymers* 23 (2010): 155–159.

10. Z. Song, M. Xing, J. Zhang, B. Li, and S. Wang, "Determination of Phase Diagram of a Ternary PVDF/γ-BL/DOP System in TIPS Process

and Its Application in Preparing Hollow Fiber Membranes for Membrane Distillation," *Separation and Purification Technology* 90 (2012): 221–230, https://doi.org/10.1016/j.seppur.2012.02.043.

11. C. H. Du, Y. Y. Xu, and B. K. Zhu, "Plasticizer Effect of Dibutyl Phthalate on the Morphology and Mechanical Properties of Hard Elastic Poly(Vinylidene Fluoride) Fibers," *Journal of Applied Polymer Science* 114 (2009): 3645–3651, https://doi.org/10.1002/app.30105.

12. B. A. Newman, J. I. Scheinbeim, and A. Sen, "The Effect of Plasticizer on the Piezoelectric Properties of Unoriented Polyvinylidene Fluoride Films," *Ferroelectrics* 57 (1984): 229–241, https://doi.org/10.1080/00150198408012765.

13. A. Marigo, C. Marega, M. Bassi, M. Fumagalli, and A. Sanguineti, "Structure and Characterization of Poly[(Vinylidene Flouride)-*co*-Hexafluoropropene]-(Dibutyl Phthalate) Blends," *Polymer International* 50 (2001): 449–455, https://doi.org/10.1002/pi.656.

14. A. Bré, M. Mollard, and M. Osgan, "Polyvinylidene Fluoride Compositions of Improved Flexibility and Their use, Particularly in the Manufacture of Flexible Tubes," 1986, US4584215.

15. P. H. C. Eilers, "A Perfect Smoother," *Analytical Chemistry* 75, no. 14 (2003): 3631–3636, https://doi.org/10.1021/ac034173t.

16. Edinburgh Instruments, *The Beer-Lambert Law* (Edinburgh Instruments, 2021).

17. P. Martins, A. C. Lopes, and S. Lanceros-Mendez, "Electroactive Phases of Poly(Vinylidene Fluoride): Determination, Processing and Applications," *Progress in Polymer Science* 39 (2014): 683–706, https://doi.org/10.1016/j.progpolymsci.2013.07.006.

18. X. Cai, T. Lei, D. Sun, and L. Lin, "A Critical Analysis of the α, β and γ Phases in Poly(Vinylidene Fluoride) Using FTIR," *RSC Advances* 7 (2017): 15382–15389, https://doi.org/10.1039/c7ra01267e.

19. M. Gu, J. Zhang, X. Wang, and W. Ma, "Crystallization Behavior of PVDF in PVDF-DMP System via Thermally Induced Phase Separation," *Journal of Applied Polymer Science* 102 (2006): 3714–3719, https://doi.org/10.1002/app.24531.

20. J. Sun, L. Yao, Q. L. Zhao, et al., "Modification on Crystallization of Poly(Vinylidene Fluoride) (PVDF) by Solvent Extraction of Poly(Methyl Methacrylate) (PMMA) in PVDF/PMMA Blends," *Frontiers of Materials Science* 5 (2011): 388–400, https://doi.org/10.1007/s11706-011-0152-2.

21. X. Zhao, J. Cheng, J. Zhang, S. Chen, and X. Wang, "Crystallization Behavior of PVDF/PMMA Blends Prepared by In Situ Polymerization From DMF and Ethanol," *Journal of Materials Science* 47 (2012): 3720–3728, https://doi.org/10.1007/s10853-011-6221-1.

22. K. Nakagawa and Y. Ishida, "Annealing Effects in Poly(Vinylidene Fluoride) as Revealed by Specific Volume Measurements, Differential Scanning Calorimetry, and Electron Microscopy," *Journal of Polymer Science Part B: Polymer Physics* 11 (1973): 2153–2171, https://doi.org/10.1002/pol.1973.180111107.

23. T. Nishiyama, T. Sumihara, E. Sato, and H. Horibe, "Effect of Solvents on the Crystal Formation of Poly (Vinylidene Fluoride) Film Prepared by a Spin-Coating Process," *Polymer Journal* 49 (2017): 319–325, https://doi.org/10.1038/pj.2016.116.

24. A. Salimi and A. A. Yousefi, "Conformational Changes and Phase Transformation Mechanisms in PVDF Solution-Cast Films," *Journal of Polymer Science Part B: Polymer Physics* 42 (2004): 3487–3495, https://doi.org/10.1002/polb.20223.

25. R. Gregorio, Jr. and M. Cestari, "Effect of Temperature on the Crystalline Phase Content and Morphology of Poly(Vinylidene Fluoride)," *Journal of Polymer Science. Part B, Polymer Physics* 32 (1994): 859–870.

26. R. Gregorio Jr and D. S. Borges, "Effect of Crystallization Rate on the Formation of the Polymorphs of Solution Cast Poly(Vinylidene Fluoride)," *Polymer* 49, no. 18 (2008): 4009–4016, https://doi.org/10.1016/j.polymer.2008.07.010.

27. M. Benz and W. B. Euler, "Determination of the Crystalline Phases of Poly(Vinylidene Fluoride) Under Different Preparation Conditions Using Differential Scanning Calorimetry and Infrared Spectroscopy," *Journal of Applied Polymer Science* 89 (2003): 1093–1100, https://doi.org/10.1002/app.12267.

28. M. Benz, W. B. Euler, and O. J. Gregory, "The Role of Solution Phase Water on the Deposition of Thin Films of Poly(Vinylidene Fluoride)," *Macromolecules* 35 (2002): 2682–2688, https://doi.org/10.1021/ma011744f.

29. R. Gregorio, Jr., "Determination of the α, β, and γ Crystalline Phases of Poly(Vinylidene Fluoride) Films Prepared at Different Conditions," *Journal of Applied Polymer Science* 100 (2006): 3272–3279, https://doi.org/10.1002/app.23137.

30. S. Satapathy, S. Pawar, P. K. Gupta, and K. B. RVarma, "Effect of Annealing on Phase Transition in Poly(Vinylidene Fluoride) Films Prepared Using Polar Solvent," *Bulletin of Materials Science* 34, no. 4 (2011): 727–733, https://doi.org/10.1007/s12034-011-0187-0.

31. P. Sajkiewicz, "Crystallization Behaviour of Poly(Vinylidene Fluoride)," *European Polymer Journal* 35 (1999): 1581–1590, https://doi.org/10.1016/S0014-3057(98)00242-0.

32. A. J. Lovinger, D. D. Davis, R. E. Cais, and J. M. Kometani, "The Role of Molecular Defects on the Structure and Phase Transitions of Poly(Vinylidene Fluoride)," *Polymer* 28 (1987): 617–626.

33. R. Gregorio and E. M. Ueno, "Effect of Crystalline Phase, Orientation and Temperature on the Dielectric Properties of Poly (Vinylidene Fluoride) (PVDF)," *Journal of Materials Science* 34 (1999): 4489–4500.

34. W. M. Prest and D. J. Luca, "The Formation of the γ Phase From the α and β Polymorphs of PVDF," *Journal of Applied Polymer Science* 49 (1978): 5042–5047, https://doi.org/10.1063/1.324439.

35. D. Wadkin-Snaith, P. A. Mulheran, and K. Johnston, "The Impact of Plasticisers on Crystal Nucleation, Growth and Melting in Linear Polymers," *Polymer* 304 (2024): 127095, https://doi.org/10.15129/3d50eb.

36. K. Pramod and R. B. Gangineni, "Influence of Solvent Evaporation Rate on Crystallization of Poly(Vinylidene Fluoride) Thin Films," *Bulletin of Materials Science* 38 (2015): 1093–1098, https://doi.org/10.1007/s12034-015-0894-z.

37. Y. Zhao, Y. Zhou, Y. Yang, J. Xu, Z. D. Chen, and Y. Jiang, "The Impact of Solvents on Properties of Solution-Cast Poly(Vinylidene Fluoride) Films for Energy Storage," *Materials Letters* 219 (2018): 201–204, https://doi.org/10.1016/j.matlet.2018.02.110.

38. K. E. Strawhecker, S. K. Kumar, J. F. Douglas, and A. Karim, "The Critical Role of Solvent Evaporation on the Roughness of Spin-Cast Polymer Films," *Macromolecules* 34 (2001): 4669–4672, https://doi.org/10.1021/ma001440d.

39. Í. López García, J. L. Keddie, and M. Sferrazza, "Probing the Early Stages of Solvent Evaporation and Relaxation in Solvent-Cast Polymer Thin Films by Spectroscopic Ellipsometry," *Surface and Interface Analysis* 43 (2011): 1448–1452, https://doi.org/10.1002/sia.3728.

40. C. Schaefer, P. Van Der Schoot, and J. J. Michels, "Structuring of Polymer Solutions Upon Solvent Evaporation," *Physical Review E: Statistical, Nonlinear, and Soft Matter Physics* 91, no. 2 (2015): 022602, https://doi.org/10.1103/PhysRevE.91.022602.

41. R. Gregorio, Jr. and R. C. Capitao, "Morphology and Phase Transition of High Melt Temperature Crystallized Poly(Vinylidene Fluoride)," *Journal of Materials Science* 35 (2000): 299–306, https://doi.org/10.1023/A.

42. A. J. Lovinger, "Crystalline Transformations in Spherulites of Poly(Vinylidene Fluoride)," *Polymer* 21 (1980): 1317–1322.

43. W. M. Prest and D. J. Luca, "The Morphology and Thermal Response of High-Temperature–Crystallized Poly(Vinylidene Fluoride)," *Journal of Applied Physics* 46 (1975): 4136–4143, https://doi.org/10.1063/1.321438.